THE JOURNAL OF BIOLOGICAL CHEMISTRY VOL. 287, NO. 32, pp. 26506–26512, August 3, 2012

Regulation of Hyperpolarization-activated Cyclic Nucleotide-gated (HCN) Channel Activity by cCMP*[S]

Received for publication, February 28, 2012, and in revised form, June 13, 2012 Published, JBC Papers in Press, June 19, 2012, DOI 10.1074/jbc.M112.357129

Xiangang Zong[‡], Stefanie Krause[‡], Cheng-Chang Chen[‡], Jens Krüger[§], Christian Gruner[‡], Xiaochun Cao-Ehlker[‡], Stefanie Fenske[‡], Christian Wahl-Schott[‡], and Martin Biel[‡1]

From the [‡]Center for Integrated Protein Science (CIPSM) and Zentrum für Pharmaforschung, Department Pharmazie, Ludwig-Maximilians-Universität München, 80539 Munich and the [§]Applied Bioinformatics Group, Wilhelm Schickard Institute for Computer Science, Eberhard Karls Universität Tübingen, 72076 Tübingen, Germany

Background: HCN channels are dually gated by membrane hyperpolarization and binding of cAMP.
Results: We identify cCMP as a novel regulator of heterologously expressed and native HCN channels.
Conclusion: HCN channels are cellular receptors for cCMP.
Significance: Modulatory effects of cCMP must be considered when studying physiological effects involving HCN channels.

Activation of hyperpolarization-activated cyclic nucleotide-gated (HCN) channels is facilitated *in vivo* by direct binding of the second messenger cAMP. This process plays a fundamental role in the fine-tuning of HCN channel activity and is critical for the modulation of cardiac and neuronal rhythmicity. Here, we identify the pyrimidine cyclic nucleotide cCMP as another regulator of HCN channels. We demonstrate that cCMP shifts the activation curves of two members of the HCN channel family, HCN2 and HCN4, to more depolarized voltages. Moreover, cCMP speeds up activation and slows down deactivation kinetics of these channels. The two other members of the HCN channel family, HCN1 and HCN3, are not sensitive to cCMP. The modulatory effect of cCMP is reversible and requires the presence of a functional cyclic nucleotide-binding domain. We determined an EC_{50} value of ~30 μM for cCMP compared with 1 μM for cAMP. Notably, cCMP is a partial agonist of HCN channels, displaying an efficacy of ~0.6. cCMP increases the frequency of pacemaker potentials from isolated sinoatrial pacemaker cells in the presence of endogenous cAMP concentrations. Electrophysiological recordings indicated that this increase is caused by a depolarizing shift in the activation curve of the native HCN current, which in turn leads to an enhancement of the slope of the diastolic depolarization of sinoatrial node cells. In conclusion, our findings establish cCMP as a gating regulator of HCN channels and indicate that this cyclic nucleotide has to be considered in HCN channel-regulated processes.

Hyperpolarization-activated cyclic nucleotide-gated (HCN)[2] ion channels play a key role in controlling excitability of neurons and heart cells (1–3). In particular, the current produced by HCN channels, called I_f in heart or I_h in neurons, is involved in the generation of sinoatrial pacemaker potentials that trigger the autonomous heartbeat (4). The four members of the HCN channel family (HCN1–4) are principally gated by membrane hyperpolarization (5–7). In addition, HCN channel activity is enhanced by direct binding of cAMP to a cyclic nucleotide-binding domain (CNBD) in the C terminus of the channels. This type of channel regulation plays an important role in a variety of physiological settings. For example, cAMP-dependent up-regulation of I_f in sinoatrial node (SAN) cells contributes to the increase in heart rate following sympathetic stimulation (8), whereas down-regulation of I_f at low cAMP levels leads to the decrease in heart rate in response to vagal stimulation (9). cAMP-dependent regulation of I_h is also implicated in the modulation of neuronal circuit activity that controls complex brain functions such as sleep phases (10), memory formation (11), and coincidence detection of sound (12).

The purine cyclic nucleotides cAMP and cGMP are well established second messengers that confer the cellular effects of a wide range of hormones and neurotransmitters. By contrast, the natural existence of the pyrimidine 3′,5′-monophosphates cCMP and cUMP has been debated (13–17). However, recent highly sensitive liquid chromatography/mass spectrometry approaches have confirmed that many cell types contain micromolar concentrations of cCMP and cUMP (18). Although a specific cCMP receptor has not yet been identified, it was shown that this cyclic nucleotide cross-activates cAMP- and cGMP-dependent protein kinases (19). In particular, cCMP was found to relax aortic smooth muscle by activating cGMP-dependent protein kinase type I (20). cCMP was also shown to inhibit platelet aggregation via cGMP-dependent protein kinase type I signaling (20). The CNBDs of cGMP-dependent protein kinases reveal strong sequence homology to the CNBDs of HCN channels (1). Given this structural relationship, we wondered whether HCN channels may be also regulated by interaction with cCMP. In support of this hypothesis, cCMP was shown to affect native I_f in excised patches from rabbit SAN cells (21). In this study, we examined the functional interaction between cCMP and each of the four HCN channel types. We

* This work was supported by grants from the Deutsche Forschungsgemeinschaft, the Graduate School Life Science Munich (LSM), and a fellowship from the Bayerische Forschungsstiftung (to C.-C. C.).
[S] This article contains supplemental Fig. S1.
[1] To whom correspondence should be addressed: Dept. Pharmazie, Pharmakologie für Naturwissenschaften, Ludwig-Maximilians-Universität München, Butenandtstr. 5-13, 81377 Munich, Germany. Tel.: 49-89-2180-77327; Fax: 49-89-2180-77326; E-mail: martin.biel@cup.uni-muenchen.de.
[2] The abbreviations used are: HCN, hyperpolarization-activated cyclic nucleotide-gated; CNBD, cyclic nucleotide-binding domain; SAN, sinoatrial node; SDD, slope of the diastolic depolarization.

also studied the co-modulation of HCN channel activity by combinations of cAMP and cCMP. Finally, we set out to study the consequences of cCMP-dependent HCN channel regulation in native SAN cells.

EXPERIMENTAL PROCEDURES

Electrophysiology in HEK293 Cells—HEK293 cell lines stably expressing murine HCN1–4 were maintained as described (22). Currents were measured from HEK293 cells stably expressing one of the four murine HCN channel types at room temperature using the whole-cell voltage-clamp technique. The extracellular solution was composed of 110 mM NaCl, 30 mM KCl, 1.8 mM $CaCl_2$, 0.5 mM $MgCl_2$, and 5 mM HEPES (pH adjusted to 7.4 with NaOH). The intracellular solution contained 130 mM KCl, 10 mM NaCl, 0.5 mM $MgCl_2$, 1 mM EGTA, 5 mM HEPES, 3 mM MgATP, and 0.5 mM NaGTP (pH adjusted to 7.4 with KOH). cAMP (Sigma), cCMP (BioLog), and cUMP (BioLog) were added to the intracellular solution at the indicated concentrations. Steady-state activation curves were determined by hyperpolarizing voltage steps from −140 to −30 mV in 10-mV increments from a holding potential of −40 mV for 1.8 s (for HCN1 and HCN2, pulse interval of 10 s) or 3.6 s (for HCN3 and HCN4, pulse interval of 20 s), followed by a step to −140 mV (see Fig. 1*A*). Currents measured immediately after the final step to −140 mV were normalized by the maximal current (I_{max}) and plotted as a function of the preceding membrane potential (see Fig. 1*A*, *arrowheads*). The data points were fitted with the Boltzmann function: $(I - I_{min})/(I_{max} - I_{min}) = (1 - \exp((V_m - V_{0.5})/k))$, where I_{min} is an offset caused by a nonzero holding current, V_m is the test potential, $V_{0.5}$ is the membrane potential for half-maximal activation, and k is the slope factor. The deactivation kinetics were measured at −40 mV following a prepulse of −140 mV, and the time constant was determined by fit with a monoexponential function starting after the initial deactivation delay.

Electrophysiology on SAN Cells—SAN cells were isolated from 6–8-week-old adult female mice using standard procedures (23). Measurements in SAN cells were performed in the whole-cell configuration. Single SAN cells were plated onto poly-L-lysine-coated coverslips. The pipette solution contained 130 mM potassium aspartate, 10 mM NaCl, 2 mM $CaCl_2$, 2 mM $MgCl_2$, 5 mM EGTA, 2 mM NaATP, 0.1 mM NaGTP, and 5 mM creatine phosphate (pH adjusted to 7.2 with KOH). I_f was recorded at room temperature in bath solution containing 138 mM NaCl, 4 mM KCl, 1 mM $CaCl_2$, 1 mM $MgCl_2$, 5 mM EGTA, 10 mM HEPES, 10 mM glucose, 2 mM $BaCl_2$, and 0.3 mM $CdCl_2$ (pH adjusted to 7.2 with NaOH). Currents were recorded by stepping from a holding potential of −35 mV to test potentials ranging from −150 to −40 mV in 10-mV increments for 5.5 s, followed by a step to −150 mV for 0.5 s before stepping back to the holding potential. Action potentials were recorded at 33 ± 0.5 °C in bath solution containing 140 mM NaCl, 5.4 mM KCl, 1 mM $MgCl_2$, 1.8 mM $CaCl_2$, 10 mM HEPES, and 10 mM glucose (pH adjusted to 7.4 with NaOH). The effect of cCMP and cAMP was tested by adding cCMP or cAMP to the pipette solution as indicated. Changes in liquid junction potentials were either calculated using JPCalc software (24) or directly measured by a free-flowing KCl electrode. The liquid junction potential was −13.9 mV for solutions used for action potential recording.

For determination of the slope of the diastolic depolarization (SDD), the local means of several (n = 25–45) successive spontaneous action potentials were averaged. The diastolic depolarization was defined as the phase of the action potential in the interval between the maximal diastolic potential and the time when the voltage derivative (dV/dt) overtakes a threshold of 0.5 mV/ms (25). In experiments involving HEK cell lines and SAN cells, data were acquired at 10 kHz using an Axopatch 200B amplifier and pCLAMP 10.2 (Molecular Devices). Voltage-clamp data were analyzed off-line using Clampfit 10.2 and Origin 6.1.

Planar Patch-clamp Technology—To examine the kinetics of HCN channel activation by intracellular cCMP, the planar patch-clamp technology combined with a fast internal perfusion system (Port-a-Patch, Nanion Technologies, Munich, Germany) was used (26). Currents were recorded using an EPC-10 patch-clamp amplifier (HEKA, Lambrecht, Germany) and PatchMaster acquisition software (HEKA). Data were digitized at 40 kHz and filtered at 2.8 kHz. Fast and slow capacitive transients were cancelled by the compensation circuit of the EPC-10 amplifier. All recordings were obtained at room temperature. The extracellular solution was composed of 110 mM NaCl, 30 mM KCl, 1.8 mM $CaCl_2$, 0.5 mM $MgCl_2$, and 5 mM HEPES (pH adjusted to 7.4 with NaOH). The intracellular solution contained 70 mM KCl, 60 mM KF, 10 mM NaCl, 0.5 mM $MgCl_2$, and 5 mM HEPES (pH adjusted to 7.4 with KOH). Currents were evoked from a holding potential of −40 mV by applying 5-s voltage pulses to −100 mV every 10 s. The effects of cyclic nucleotides were examined by exchanging the standard internal solution with internal solutions supplemented with either cCMP or cAMP using the internal perfusion system. To monitor the time course of HCN channel rundown, the cells were internally perfused with the standard internal solution without cyclic nucleotides.

Modeling—The crystal structures of CNBDs of murine HCN2 and human HCN4 were used (Protein Data Bank codes 1Q43 and 3U11) as receptors for docking (27, 28). Calculations were carried out with MOE (Molecular Operating Environment) 2010.10 (Chemical Computing Group, Montreal, Canada). The binding site selection was based on the Site Finder module of MOE, marking the cyclic nucleotide-binding pocket with dummy atoms (29). Different ligand placement methods available in MOE (Triangle Matcher, Alpha PMI, and Alpha Triangle) were used to estimate the binding energies of cAMP and cCMP toward HCN2 and HCN4. Binding affinities were estimated with the London dG scoring function after a force field-based refinement and rescoring. During refinement, a tethered rearrangement of side chains within 6 Å of the ligand was allowed. The MMFF94s force field with a generalized Born solvation model was used for all docking calculations. Plots and figures were created with MOE.

Statistics—For electrophysiological data, statistical analysis was performed by one-way analysis of variance. Data are presented as means ± S.E. (n = number of recorded cells). Values of $p < 0.05$ were considered significant.

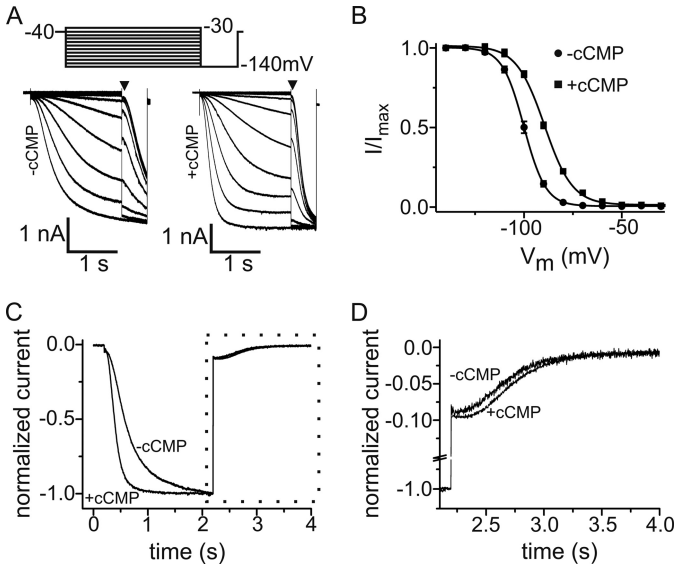

FIGURE 1. **Modulation of HCN2 current by cCMP.** *A*, voltage step protocol and family of current traces of HEK293 cells stably expressing HCN2 without (*left*) and with (*right*) 1 mM cCMP in the pipette solution. *B*, normalized activation curves of HCN2 in the presence (■) and absence (●) of 1 mM cCMP. The *solid lines* are the fits to the Boltzmann equation with the following parameters: in the absence of cCMP ($n = 15$), $V_{0.5} = -102$ mV and $k = 6.34$ mV; and in the presence of cCMP ($n = 14$), $V_{0.5} = -93.8$ mV and $k = 6.53$ mV. *C*, normalized current traces of HCN2 in the absence and presence of 1 mM cCMP. Currents were evoked by a hyperpolarizing step to −140 mV from a holding potential of −40 mV, followed by a voltage pulse to −40 mV. Maximal currents at −140 mV were normalized. *D*, display of current traces during HCN2 channel deactivation at −40 mV (area within the *dotted box* in *C*).

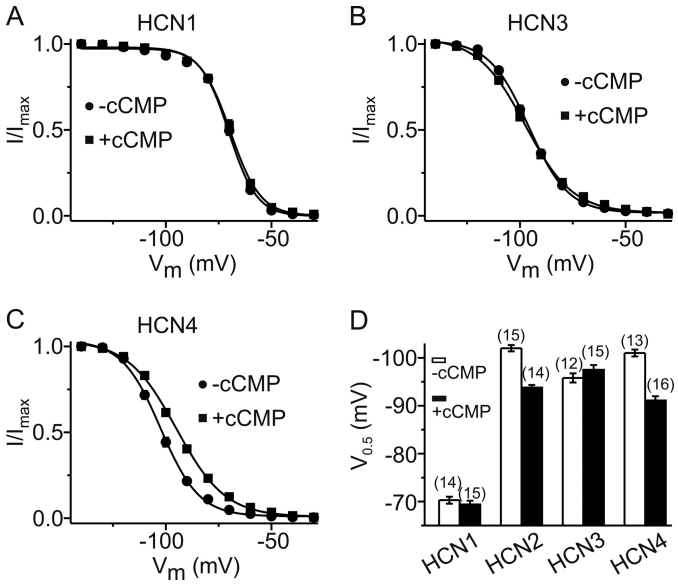

FIGURE 2. **Effect of cCMP on activation of HCN channels.** *A–C*, activation curves of HCN1 (*A*), HCN3 (*B*) and HCN4 (*C*) in the presence (■) and absence (●) of 1 mM cCMP. The *solid lines* are the fits to the Boltzmann equation with the following parameters: for HCN1 in the absence of cCMP ($n = 14$), $V_{0.5} = -70.2$ mV and $k = 6.57$ mV; for HCN1 in the presence of cCMP ($n = 15$), $V_{0.5} = -69.5$ mV and $k = 7.09$ mV; for HCN3 in the absence of cCMP ($n = 12$), $V_{0.5} = -95.8$ mV and $k = 9.30$ mV; for HCN3 in the presence of cCMP ($n = 15$), $V_{0.5} = -97.5$ mV and $k = 11.2$ mV; for HCN4 in the absence of cCMP ($n = 16$), $V_{0.5} = -101$ mV and $k = 9.71$ mV; and for HCN4 in the presence of cCMP ($n = 15$), $V_{0.5} = -91.1$ mV and $k = 12.3$ mV. *D*, summarized $V_{0.5}$ data of the four HCN channels in the absence (*white bars*) and presence (*black bars*) of 1 mM cCMP. The $V_{0.5}$ shift induced by cCMP in HCN2 and HCN4 is highly significant ($p < 0.001$).

RESULTS

Regulation of HCN2- and HCN4-mediated Currents by cCMP—We studied the effect of cCMP on I_h in a HEK293 cell line stably expressing HCN2 (Fig. 1). Fig. 1*A* shows representative families of current traces measured in the whole-cell mode under control conditions and after intracellular application of 1 mM cCMP via the patch pipette. cCMP had two effects on the HCN2-mediated current. First, it shifted the voltage dependence of activation to ~8 mV more positive values ($V_{0.5(-cCMP)} = -102 \pm 0.67$ mV ($n = 15$) and $V_{0.5(+cCMP)} = -93.8 \pm 0.54$ mV ($n = 14$)) (Fig. 1*B*). Second, cCMP affected the activation and deactivation kinetics of the current. In the presence of cCMP, the current activated significantly faster than in the absence of cCMP (τ_{act} at −140 mV = 185 ± 9.3 ms ($n = 14$) *versus* 307 ± 10.5 ms ($n = 15$) in the absence of cCMP) (Fig. 1*C*). As expected for the action of a gating activator, deactivation at −40 mV was slower in the presence of cCMP (τ_{deact} at −40 mV = 462 ± 23.5 ms ($n = 13$) *versus* 363 ± 23 ms ($n = 15$) in the absence of cCMP) (Fig. 1, *C* and *D*).

Among the four members of the HCN channel family, only HCN2 and HCN4 are profoundly regulated by cAMP, whereas HCN1 and HCN3 are only weakly sensitive (if at all) to cAMP (1). We tested whether a similar range of sensitivity is also seen for cCMP. Indeed, there was no significant effect of cCMP on the $V_{0.5}$ of HCN1 (Fig. 2, *A* and *D*) and HCN3 (Fig. 2, *B* and *D*). In contrast, cCMP shifted the $V_{0.5}$ of HCN4 to a comparable extent (about +10 mV) as observed for HCN2 (Fig. 2, *C* and *D*). cUMP, which is chemically closely related to cCMP, activated HCN2 and HCN4 in a comparable way as cCMP (supplemental Fig. S1).

Purine cyclic nucleotides activate HCN channels by binding in a reversible way to the intracellular CNBD. We tested whether cCMP exerts its effects in a similar manner. To this end, we measured currents from a HEK293 cell line stably expressing HCN4 using a planar patch-clamp setup (Port-a-Patch) that allows rapid internal perfusion and washout of solutions. Both cAMP (Fig. 3*A*) and cCMP (Fig. 3*B*) led to a profound increase in the current at −100 mV that was fully reversible after washout. However, although a 100-fold higher concentration was used for cCMP than for cAMP (100 *versus* 1 μM), the maximal increase in the current amplitude obtained with cCMP was significantly smaller than that obtained with cAMP (~1.3-fold for cCMP *versus* 1.7-fold for cAMP at −100 mV). The drop in the current amplitude below the initial level after washout of the cyclic nucleotides was caused by HCN channel rundown. It occurred to the same extent when the cells were perfused with internal solution without cyclic nucleotides (Fig. 3, *A* and *B*). The weaker effect of cCMP was also reflected in the extent of the shift in $V_{0.5}$, which was +10.2 ± 1.11 mV for 100 μM cAMP ($n = 7$; $V_{0.5(-cAMP)} = -111 \pm 4.24$ mV and $V_{0.5(+cAMP)} = -101 \pm 3.32$ mV) and +5.6 ± 0.67 mV for 100 μM cCMP ($n = 8$; $V_{0.5(-cCMP)} = -110 \pm 2.32$ mV and $V_{0.5(+cCMP)} = -105 \pm 2.56$ mV). The more negative $V_{0.5}$ values obtained with the planar patch-clamp technique (Fig. 3, *C* and *D*) compared with the conventional whole-cell mode (Fig. 2, *C* and *D*) probably reflect the fact that phosphatidylinositol 4,5-bisphosphate, an important coactivator of HCN channel gating, is washed out during the internal perfusion in the planar patch-

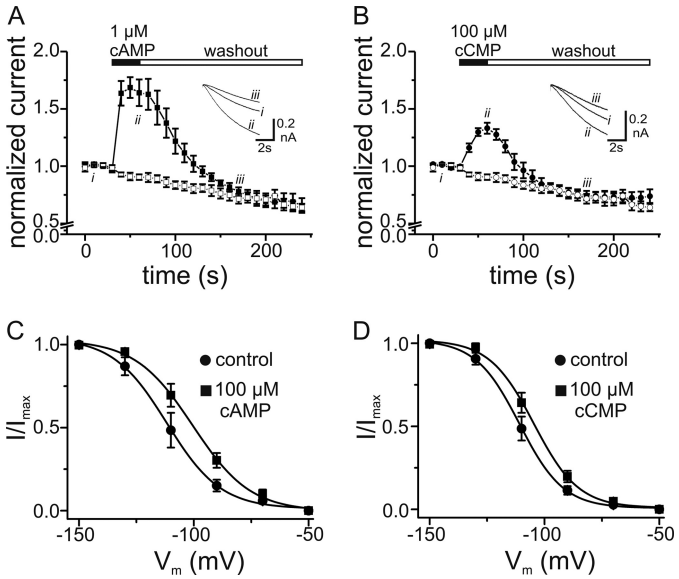

FIGURE 3. **Effects of cCMP and cAMP on HCN4 currents determined upon internal perfusion with planar patch-clamp system.** *A*, time course of HCN4 currents from five cells recorded during a series of 6-s hyperpolarizing pulses from −40 to −100 mV. Currents were measured 3 s after the beginning of individual hyperpolarizing pulses and normalized to the current before application of 1 μM cAMP (■). Application and washout of cAMP are indicated by *closed* and *open bars*, respectively. HCN channel rundown without application of cAMP was monitored (□). *Inset*, current traces recorded at the indicated time points. *B*, time course of HCN4 currents recorded from six cells with application of 100 μM cCMP (●). The protocol was as described for *A*. HCN channel rundown was monitored without application of cCMP (○). *C*, activation curves of HCN4 before and 15 s after internal application of 100 μM cAMP. The *solid lines* are the fits of a Boltzmann function to the data with the following values: $V_{0.5} = -112$ mV and $k = 11.7$ mV for the control and $V_{0.5} = -100$ mV and $k = 12.6$ for cAMP ($n = 7$). *D*, activation curves of HCN4 before and 15 s after internal application of 100 μM cCMP. The *solid lines* are fits of a Boltzmann function to the data with the following values: $V_{0.5} = -111$ mV and $k = 9.55$ mV for the control and $V_{0.5} = -105$ mV and $k = 9.69$ mV for cCMP ($n = 8$).

clamp measurements, similar to what is observed for the excised inside-out patch configuration (30–32).

Interaction of cCMP with the CNBDs of HCN Channels—We used computer-based docking approaches to examine the binding of cCMP and cAMP to the crystal structures of the CNBDs of HCN2 (27) and HCN4 (28, 33, 34). Fig. 4 (*A* and *B*) shows molecular surface illustrations of the HCN2 CNBD with either cAMP or cCMP. There was no principal difference in the analogous models for HCN4 (data not shown). The residues of the CNBD that interacts with cyclic nucleotides are same for cCMP and cAMP. Specific interactions of Arg-591 and Thr-592 with the phosphor-bound oxygens of the sugar moiety and between the hydroxyl group and Gly-581/Glu-582 are observed (*dashed blue lines*). The aromatic part of the ligand interacts with Val-564 and Arg-632. The non-polar hydrogen atoms of Arg-632 potentially contribute to π stacking of cAMP more than cCMP (*dashed red lines*). Less specific interactions are observed for Ile-545, Leu-574, Phe-580, Ile-583, Cys-584, Ala-593, and Val-595 (data not shown). Three different placement methods (see "Experimental Procedures") were used to estimate the difference in binding energies. A lower affinity was estimated for cCMP than for cAMP ($\Delta\Delta G = 0.53$ kcal/mol for HCN2 and 1.46 kcal/mol for HCN4), averaging over the three methods. In agreement with this difference, the apparent experimental affinity of cCMP was ~30 times lower than that of cAMP (for HCN2, $EC_{50(cCMP)} = 29$ μM and $EC_{50(cAMP)} = 1$ μM) (Fig. 5, *A* and *B*). Moreover, in agreement with the planar patch-clamp measurements, the maximal shift in $V_{0.5}$ by cCMP at the saturating concentration was only ~60% of that by cAMP (Fig. 5*B*). Together, these results suggest that cCMP is a partial agonist of HCN channels. To confirm this hypothesis, we measured the effect of cCMP in the presence of cAMP (Fig. 5, *C–F*) on heterologously expressed HCN2 channels. As expected for a partial agonist, saturating concentrations of cCMP, when applied together with high concentrations of cAMP, led to a slight but highly significant hyperpolarizing shift in $V_{0.5}$ compared with the $V_{0.5}$ seen with high concentrations of cAMP alone (shifts in $V_{0.5}$ of 12.6 ± 0.6 mV with 10 μM cAMP, 8.56 ± 0.5 mV with 10 μM cAMP and 1 mM cCMP, and 7.7 ± 0.5 mV with 1 mM cCMP) (Fig. 5, *A*, *C* and *D*). The cyclic nucleotides exerted an additive effect on the activation of HCN channels when both were applied together at lower concentrations, around their respective EC_{50} values. Under these conditions, $V_{0.5}$ was shifted to more depolarized potentials compared with the application of cAMP alone (shifts in $V_{0.5}$ of 5.8 ± 0.7 mV with 1 μM cAMP, 7.0 ± 0.5 mV with 50 μM cCMP, and 10.0 ± 0.8 mV with 1 μM cAMP and 50 μM cCMP) (Fig. 5, *E* and *F*). To exclude that cCMP effects result from interactions with residues outside of the CNBD, we determined the activation curve in an HCN2 mutant that is deficient for cAMP binding due to the presence of R591E and T592A (HCN2(R591E/T592A)) (Fig. 5, *G* and *H*) (34). In this mutant cCMP, no longer led to a shift in $V_{0.5}$, indicating that an intact CNBD is required for conferring the modulatory action of cCMP.

cCMP Increases the Frequency of Sinoatrial Pacemaker Potentials—We wondered whether cCMP modulation of HCN channels could exert physiological effects *in vivo*. To this end, we determined the effect of cCMP on sinoatrial pacemaking (Fig. 6). Fig. 6*A* shows representative pacemaker potentials of murine SAN cells under control conditions and after intracellular application of 1 mM cCMP or cAMP via the patch pipette. Both cyclic nucleotides significantly increased the firing rate of pacemaker potentials (Fig. 6, *A* and *B*). The effect was quantitatively stronger for cAMP than for cCMP (increase of 46 ± 5% *versus* 19 ± 5% by 1 mM cAMP or cCMP, respectively). In agreement with the partial agonistic nature of cCMP, the increase in the firing frequency induced by co-application of saturating cCMP and cAMP concentrations was smaller than that observed with cAMP alone (357.6 ± 9 beats/min ($n = 9$) with 10 μM cAMP + 1 mM cCMP *versus* 393.0 ± 12.7 beats/min with 10 μM cAMP ($n = 10$); $p < 0.05$). Like cAMP, cCMP enhanced the frequency of pacemaker potentials by increasing the SDD (Fig. 6, *C* and *D*). As observed for HCN4, which is the principal HCN channel isoform underlying cardiac I_f (35), cCMP shifted the activation curve of I_f by about +5 mV, which is somewhat less than the shift induced by saturating cAMP (+10 mV) (Fig. 6, *E* and *F*).

DISCUSSION

Here, we have demonstrated that the pyrimidine cyclic nucleotide cCMP is an activator of HCN channel gating. Within the HCN channel family, HCN2 and HCN4, the two channels that are also known to be regulated by cAMP and

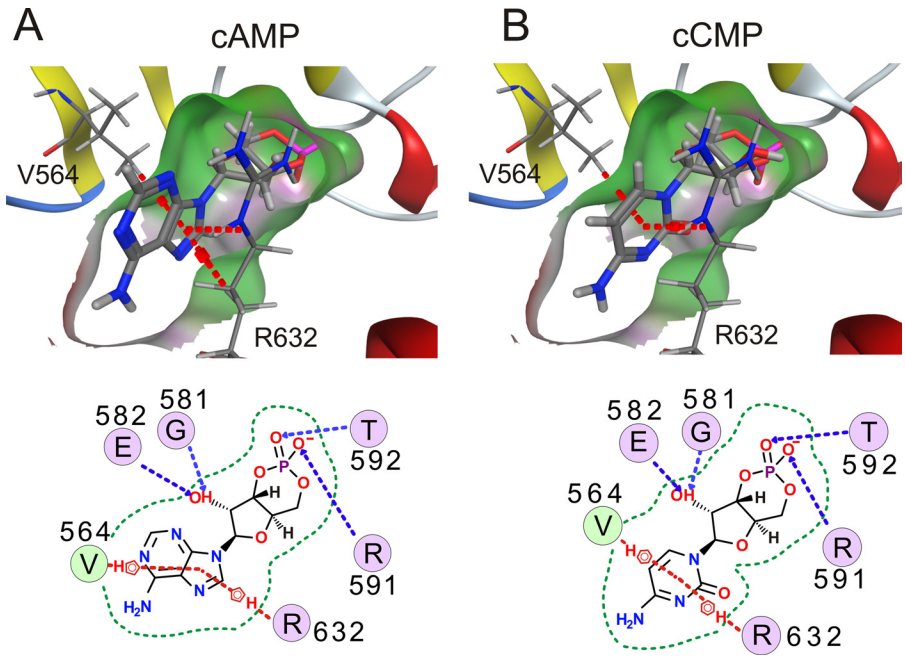

FIGURE 4. **cCMP binds to CNBD of HCN2 channels.** Structural models of a portion of the CNBD of HCN2 with bound cAMP (*A*) and cCMP (*B*) are shown (*upper*). The pocket is visualized by a molecular surface (hydrophobic (*green*) and hydrogen bonding (*magenta*)). Interactions between the protein and cyclic nucleotide are shown schematically (*lower*). *Dashed lines* indicate π stacking (*red*) and hydrogen bonding (*blue*). The border of the binding pocket is marked by *dashed green lines*.

cGMP, displayed profound regulation by cCMP. In contrast, gating of HCN1 and HCN3 was not affected by cCMP. cCMP induced a shift in the HCN2 and HCN4 activation curves by about +6–8 mV. This voltage shift is significantly smaller than that observed for cAMP (+10–12 mV), suggesting that cCMP is a partial agonist of HCN channels. In agreement with this model, in HCN2, cCMP diminished the maximal voltage shift induced by cAMP when co-applied with cAMP. Beside its effects on the voltage dependence of activation, cCMP affected gating kinetics. Like cAMP, cCMP accelerated the speed of activation, whereas it slowed down channel deactivation. On a structural level, the stimulatory effect of cCMP requires the presence of a functional CNBD because it was completely lost if two key residues that are required for cyclic nucleotide binding were mutated (R591E/T592A in HCN2). Our docking experiments suggest that cCMP interacts with the same principal residues within the CNBDs of HCN2 and HCN4 as cAMP. The apparent affinities determined in our electrophysiological experiments are ~1 μM for cAMP and 30 μM for cCMP, thus yielding an approximate difference of $\Delta\Delta G = 2.0$ kcal/mol. The computational estimate of 0.5–1.5 kcal/mol determined in docking experiments matches this value quite well. It should be noted that docking approaches in general can hardly take the flexibility of the binding pocket into account, including rearrangements after ligand binding, as they are well documented for other cyclic nucleotide-binding proteins (36–38). Furthermore, it is difficult to estimate absolute binding energies, as scoring functions are always calibrated to a specific training set. Nevertheless, the good agreement found in our study gives great confidence that the binding mode of the ligands and their relative difference in affinity are produced correctly. In our docking model, the anchoring of the sugar moieties within the binding pocket of HCN2 or HCN4 is almost identical for cAMP and cCMP. The observed difference in binding affinity most likely is based on how the delocalized π systems (38) of cAMP and cCMP interact with hydrophobic parts of Val-564 and Arg-632. Consequently, the ligand is shifted slightly within the binding pocket, allowing a slightly better fit for cAMP than for cCMP. Molecular dynamics simulation in combination with mutagenesis demonstrated that Arg-632 is essential for high ligand efficacy due to its selective stabilization of cyclic nucleotide binding to the open channel (39). Thus, it is tempting to speculate that the somewhat weaker interaction of Arg-632 with cCMP compared with cAMP may explain why cCMP is only a partial agonist of HCN channels.

The physiological relevance of cCMP is currently discussed controversial. So far, specific enzymes that synthesize or degrade cCMP have not been identified. However, there is recent evidence that soluble guanylyl cyclases possess the capacity to synthesize cCMP in the presence of the activator nitric oxide (40). Moreover, it was shown that cCMP can relax vascular smooth muscle and inhibit platelet activation via activation of cyclic nucleotide-dependent protein kinases (19–20). The exact concentrations of cCMP and cUMP in intact tissues have not been determined. However, in cell lines from various species and tissue origins, cCMP concentrations under basal conditions are in the same range as cGMP concentrations, ranging from 30 to 70 μM (18). These concentrations are well in the range required to modulate HCN channel activity ($EC_{50(cCMP)}$ = 30 μM). In support of a physiological role of cCMP, we have shown that this cyclic pyrimidine has the potential to increase heart rate by activating sinoatrial I_f and thereby enhance the SDD in SAN pacemaker cells. In this context, it is important to note that owing to its partial agonistic activity, cCMP action could be complex in a physiological setting. If present alone, cCMP is an activator of HCN channel

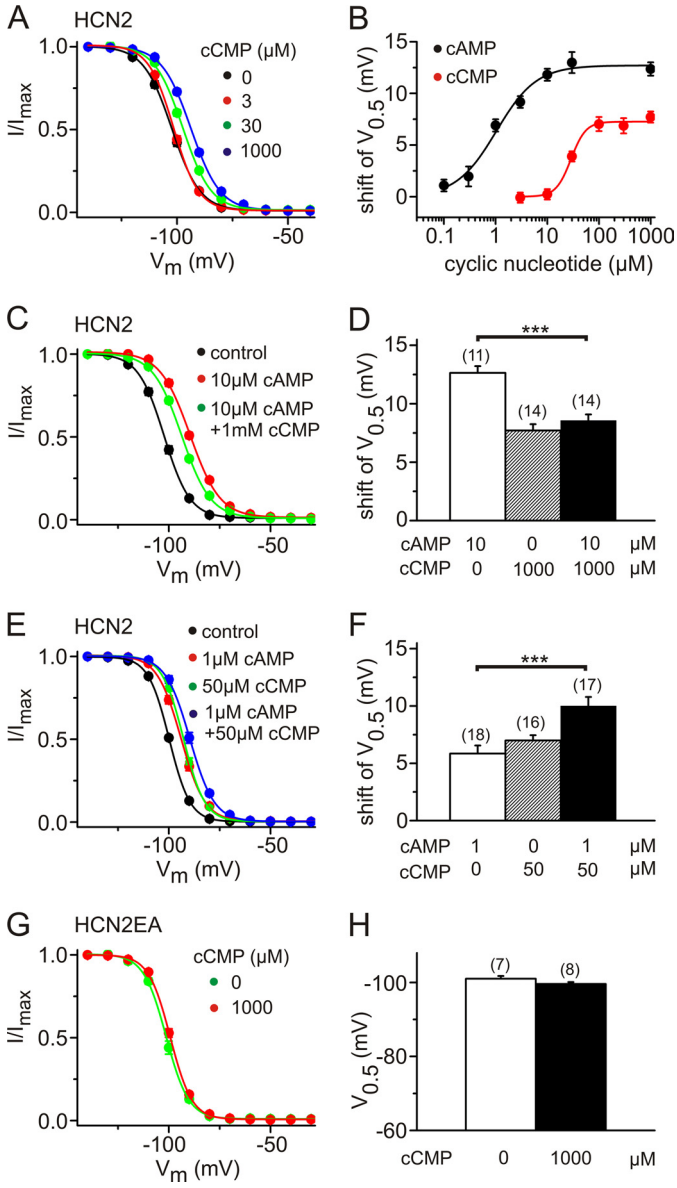

FIGURE 5. **cAMP and cCMP display different gating efficacies in HCN2.** *A*, activation curves of HCN2 for different cCMP concentrations as indicated. *B*, shift in $V_{0.5}$ *versus* concentrations of cAMP (*black circles*) and cCMP (*red circles*) for HCN2. Data represent means ± S.E. of 7–19 cells. *C*, activation curves of HCN2 in the absence of cyclic nucleotides (*black circles*), in the presence of 10 μM cAMP (*red circles*), and in the presence of 10 μM cAMP + 1 mM cCMP (*green circles*). *D*, shift in the activation curves from the experiments shown in *A* and *C*. *E*, activation curves of HCN2 in the absence of cyclic nucleotides (*black circles*), in the presence of 1 μM cAMP (*red circles*), in the presence of 50 μM cCMP (*green circles*), and in the presence of 1 μM cAMP + 50 μM cCMP (*blue circles*). *F*, shift in the activation curves from the experiments shown in *E*. *G*, activation curve of an HCN2 mutant with an impaired CNBD (HCN2(R591E/T592A) (*HCN2EA*)) in the absence (*green circles*) and presence (*red circles*) of 1000 μM cCMP. *H*, $V_{0.5}$ values for the experiments shown in *G*. ***, $p < 0.001$.

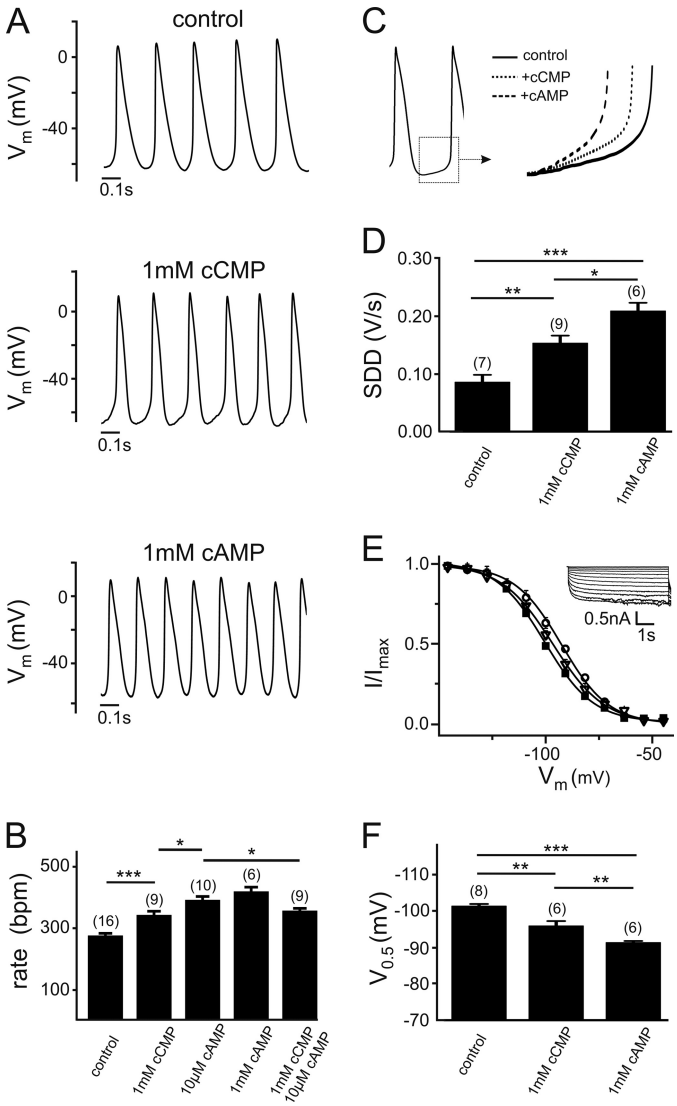

FIGURE 6. **Regulation of sinoatrial pacemaking by cCMP.** *A*, representative spontaneous action potentials of murine SAN cells recorded with the control intracellular solution or the intracellular solution containing cCMP or cAMP. *B*, firing rate with the control intracellular solution or the intracellular solution containing cAMP and/or cCMP at the concentrations indicated. *C*, increase in the SDD induced by cAMP and cCMP. *D*, quantification of the effect of cAMP and cCMP on the SDD. *E* and *F*, steady-state activation curves (*E*) and $V_{0.5}$ values (*F*) of SAN cell I_f measured in the absence of cyclic nucleotides (■) or in presence of either cCMP (▽) or cAMP (○). A typical family of I_f traces obtained from murine SAN cells is shown in the *inset* in *E*. The numbers of tested cells are given in *parentheses* in *B*, *D*, and *F*. *, $p < 0.05$; **, $p < 0.01$; ***, $p < 0.001$.

gating. If cCMP and cAMP are both present in the microenvironment of an HCN channel complex, cCMP could either enhance or dampen cAMP effects depending on the actual concentrations of both cyclic nucleotides. It should also be considered that cCMP could exert some of its physiological effects by activating PKA (19). For example, phosphorylation of calcium channels ($Ca_v1.3$), ryanodine receptors, or phospholamban by PKA would also accelerate diastolic depolarization (for review, see Ref. 41). In neuronal circuits involving HCN channel activity, cCMP up-regulation of I_h may also be relevant. Further studies will be required to dissect the specific contribution of cAMP- and cCMP-dependent regulation of HCN channel activity. To this end, it will be necessary to determine the formation and degradation of cyclic nucleotides at high temporal and spatial resolution. This work provides an important basis for such follow-up studies because it indicates that cCMP effects must be taken into account to obtain a comprehensive view of physiological processes involving HCN channels.

Acknowledgment—We thank B. Noack for excellent technical assistance.

REFERENCES

1. Biel, M., Wahl-Schott, C., Michalakis, S., and Zong, X. (2009) Hyperpolarization-activated cation channels: from genes to function. *Physiol. Rev.* **89,** 847–885
2. DiFrancesco, D. (2010) The role of the funny current in pacemaker activity. *Circ. Res.* **106,** 434–446
3. Frère, S. G., Kuisle, M., and Lüthi, A. (2004) Regulation of recombinant and native hyperpolarization-activated cation channels. *Mol. Neurobiol.* **30,** 279–305
4. Brown, H., and Difrancesco, D. (1980) Voltage-clamp investigations of membrane currents underlying pacemaker activity in rabbit sinoatrial node. *J. Physiol.* **308,** 331–351
5. Ludwig, A., Zong, X., Jeglitsch, M., Hofmann, F., and Biel, M. (1998) A family of hyperpolarization-activated mammalian cation channels. *Nature* **393,** 587–591
6. Santoro, B., Liu, D. T., Yao, H., Bartsch, D., Kandel, E. R., Siegelbaum, S. A., and Tibbs, G. R. (1998) Identification of a gene encoding a hyperpolarization-activated pacemaker channel of brain. *Cell* **93,** 717–729
7. Gauss, R., Seifert, R., and Kaupp, U. B. (1998) Molecular identification of a hyperpolarization-activated channel in sea urchin sperm. *Nature* **393,** 583–587
8. Brown, H. F., DiFrancesco, D., and Noble, S. J. (1979) How does adrenaline accelerate the heart? *Nature* **280,** 235–236
9. DiFrancesco, D., Ducouret, P., and Robinson, R. B. (1989) Muscarinic modulation of cardiac rate at low acetylcholine concentrations. *Science* **243,** 669–671
10. McCormick, D. A., and Bal, T. (1997) Sleep and arousal: thalamocortical mechanisms. *Annu. Rev. Neurosci.* **20,** 185–215
11. Wang, M., Ramos, B. P., Paspalas, C. D., Shu, Y., Simen, A., Duque, A., Vijayraghavan, S., Brennan, A., Dudley, A., Nou, E., Mazer, J. A., McCormick, D. A., and Arnsten, A. F. (2007) α2A-Adrenoceptors strengthen working memory networks by inhibiting cAMP-HCN channel signaling in prefrontal cortex. *Cell* **129,** 397–410
12. Shaikh, A. G., and Finlayson, P. G. (2005) Excitability of auditory brainstem neurons, *in vivo*, is increased by cyclic AMP. *Hear. Res.* **201,** 70–80
13. Anderson, T. R. (1982) Cyclic cytidine 3′,5′-monophosphate (cCMP) in cell regulation. *Mol. Cell. Endocrinol.* **28,** 373–385
14. Cech, S. Y., and Ignarro, L. J. (1977) Cytidine 3′,5′-monophosphate (cyclic CMP) formation in mammalian tissues. *Science* **198,** 1063–1065
15. Gaion, R. M., and Krishna, G. (1979) Cytidylate cyclase: the product isolated by the method of Cech and Ignarro is not cytidine 3′,5′-monophosphate. *Biochem. Biophys. Res. Commun.* **86,** 105–111
16. Newton, R. P., Salih, S. G., Salvage, B. J., and Kingston, E. E. (1984) Extraction, purification, and identification of cytidine 3′,5′-cyclic monophosphate from rat tissues. *Biochem. J.* **221,** 665–673
17. Newton, R. P., Kingston, E. E., Hakeem, N. A., Salih, S. G., Beynon, J. H., and Moyse, C. D. (1986) Extraction, purification, identification, and metabolism of 3′,5′-cyclic UMP, 3′,5′-cyclic IMP, and 3′,5′-cyclic dTMP from rat tissues. *Biochem. J.* **236,** 431–439
18. Burhenne, H., Beste, K. Y., Spangler, C. M., Voigt, U., Kaever, V., and Seifert, R. (2011) Determination of cytidine 3′,5 ′-cyclic monophosphate and uridine 3′,5 ′-cyclic monophosphate in mammalian cell systems and in human urine by high-performance liquid chromatography/mass spectrometry. *Naunyn-Schmiedeberg's Arch. Pharmacol.* **383,** 33
19. Wolter, S., Golombek, M., and Seifert, R. (2011) Differential activation of cAMP- and cGMP-dependent protein kinases by cyclic purine and pyrimidine nucleotides. *Biochem. Biophys. Res. Commun.* **415,** 563–566
20. Desch, M., Schinner, E., Kees, F., Hofmann, F., Seifert, R., and Schlossmann, J. (2010) Cyclic cytidine 3′,5′-monophosphate (cCMP) signals via cGMP kinase I. *FEBS Lett.* **584,** 3979–3984
21. DiFrancesco, D., and Tortora, P. (1991) Direct activation of cardiac pacemaker channels by intracellular cyclic AMP. *Nature* **351,** 145–147
22. Zong, X., Eckert, C., Yuan, H., Wahl-Schott, C., Abicht, H., Fang, L., Li, R., Mistrik, P., Gerstner, A., Much, B., Baumann, L., Michalakis, S., Zeng, R., Chen, Z., and Biel, M. (2005) A novel mechanism of modulation of hyperpolarization-activated cyclic nucleotide-gated channels by Src kinase. *J. Biol. Chem.* **280,** 34224–34232
23. Herrmann, S., Stieber, J., Stöckl, G., Hofmann, F., and Ludwig, A. (2007) HCN4 provides a "depolarization reserve" and is not required for heart rate acceleration in mice. *EMBO J.* **26,** 4423–4432
24. Barry, P. H. (1994) JPCalc, a software package for calculating liquid junction potential corrections in patch-clamp, intracellular, epithelial, and bilayer measurements and for correcting junction potential measurements. *J. Neurosci. Methods* **51,** 107–116
25. Bucchi, A., Baruscotti, M., Robinson, R. B., and DiFrancesco, D. (2007) Modulation of rate by autonomic agonists in SAN cells involves changes in diastolic depolarization and the pacemaker current. *J. Mol. Cell. Cardiol.* **43,** 39–48
26. Brüggemann, A., Stoelzle, S., George, M., Behrends, J. C., and Fertig, N. (2006) Microchip technology for automated and parallel patch-clamp recording. *Small* **2,** 840–846
27. Zagotta, W. N., Olivier, N. B., Black, K. D., Young, E. C., Olson, R., and Gouaux, E. (2003) Structural basis for modulation and agonist specificity of HCN pacemaker channels. *Nature* **425,** 200–205
28. Lolicato, M., Nardini, M., Gazzarrini, S., Möller, S., Bertinetti, D., Herberg, F. W., Bolognesi, M., Martin, H., Fasolini, M., Bertrand, J. A., Arrigoni, C., Thiel, G., and Moroni, A. (2011) Tetramerization dynamics of C-terminal domain underlies isoform-specific cAMP gating in hyperpolarization-activated cyclic nucleotide-gated channels. *J. Biol. Chem.* **286,** 44811–44820
29. Liang, J., Edelsbrunner, H., Fu, P., Sudhakar, P. V., and Subramaniam, S. (1998) Analytical shape computation of macromolecules. II. Inaccessible cavities in proteins. *Proteins* **33,** 18–29
30. Pian, P., Bucchi, A., Decostanzo, A., Robinson, R. B., and Siegelbaum, S. A. (2007) Modulation of cyclic nucleotide-regulated HCN channels by PIP_2 and receptors coupled to phospholipase C. *Pflugers Arch.* **455,** 125–145
31. Zolles, G., Klöcker, N., Wenzel, D., Weisser-Thomas, J., Fleischmann, B. K., Roeper, J., and Fakler, B. (2006) Pacemaking by HCN channels requires interaction with phosphoinositides. *Neuron* **52,** 1027–1036
32. Pian, P., Bucchi, A., Robinson, R. B., and Siegelbaum, S. A. (2006) Regulation of gating and rundown of HCN hyperpolarization-activated channels by exogenous and endogenous PIP_2. *J. Gen. Physiol.* **128,** 593–604
33. Xu, X., Vysotskaya, Z. V., Liu, Q., and Zhou, L. (2010) Structural basis for the cAMP-dependent gating in the human HCN4 channel. *J. Biol. Chem.* **285,** 37082–37091
34. Chen, S., Wang, J., and Siegelbaum, S. A. (2001) Properties of hyperpolarization-activated pacemaker current defined by coassembly of HCN1 and HCN2 subunits and basal modulation by cyclic nucleotide. *J. Gen. Physiol.* **117,** 491–504
35. Ludwig, A., Zong, X., Stieber, J., Hullin, R., Hofmann, F., and Biel, M. (1999) Two pacemaker channels from human heart with profoundly different activation kinetics. *EMBO J.* **18,** 2323–2329
36. Schünke, S., Stoldt, M., Lecher, J., Kaupp, U. B., and Willbold, D. (2011) Structural insights into conformational changes of a cyclic nucleotide-binding domain in solution from *Mesorhizobium loti* K1 channel. *Proc. Natl. Acad. Sci. U.S.A.* **108,** 6121–6126
37. Schünke, S., Stoldt, M., Novak, K., Kaupp, U. B., and Willbold, D. (2009) Solution structure of the *Mesorhizobium loti* K1 channel cyclic nucleotide-binding domain in complex with cAMP. *EMBO Rep.* **10,** 729–735
38. Rozas, I., Alkorta, I., and Elguero, J. (1997) Unusual hydrogen bonds: H$\cdots\pi$ interactions. *J. Phys. Chem. A* **101,** 9457–9463
39. Zhou, L., and Siegelbaum, S. A. (2007) Gating of HCN channels by cyclic nucleotides: residue contacts that underlie ligand binding, selectivity, and efficacy. *Structure* **15,** 655–670
40. Beste, K. Y., Burhenne, H., Kaever, V., Stasch, J. P., and Seifert, R. (2012) Nucleotidyl Cyclase Activity of Soluble Guanylyl Cyclase $\alpha_1\beta_1$. *Biochemistry* **51,** 194–204
41. Mangoni, M. E., and Nargeot, J. (2008) Genesis and regulation of the heart automaticity. *Physiol. Rev.* **88,** 919–982